Anatoly R. Melnikov*, Vladimir N. Verkhovlyuk, Evgeny V. Kalneus, Valeri V. Korolev, Vsevolod I. Borovkov, Peter S. Sherin, Maria P. Davydova, Sergei F. Vasilevsky and Dmitri V. Stass

Estimation of the Fraction of Spin-Correlated Radical Ion Pairs in Irradiated Alkanes using Magnetosensitive Recombination Luminescence from Exciplexes Generated upon Recombination of a Probe Pair

DOI 10.1515/zpch-2016-0819
Received June 14, 2016; accepted August 26, 2016

Abstract: We suggest a convenient probe exciplex system for studies in radiation spin chemistry based on a novel acceptor-substituted diphenylacetylene, 1-(phenylethynyl)-4-(trifluoromethyl)benzene that has a very short fluorescence lifetime (<200 ps) and low quantum yield (0.01) of intrinsic emission, provides efficient electron capture in alkanes and efficient exciplex formation upon recombination in pair with DMA radical cation, while exhibiting a shifted to red exciplex emission band as compared to the parent system DMA – diphenylacetylene. After chemical, luminescent, radiation and spin-chemical characterization of the new system we used the magnitude of magnetic field effect in its exciplex emission band for experimental estimation of the fraction of spin-correlated radical ion pairs under X-irradiation with upper energy cutoff 40 keV in a set of 11 alkanes. For linear and branched alkanes magnetic field effects and the corre-

***Corresponding author: Anatoly R. Melnikov,** Voevodsky Institute of Chemical Kinetics and Combustion SB RAS, 3, Institutskaya Str., 630090 Novosibirsk, Russian Federation; and Novosibirsk State University, 2, Pirogova Str., 630090 Novosibirsk, Russian Federation, e-mail: melnikov@kinetics.nsc.ru
Vladimir N. Verkhovlyuk, Evgeny V. Kalneus, Valeri V. Korolev: Voevodsky Institute of Chemical Kinetics and Combustion SB RAS, 3, Institutskaya Str., 630090 Novosibirsk, Russian Federation
Vsevolod I. Borovkov, Maria P. Davydova, Sergei F. Vasilevsky and Dmitri V. Stass: Voevodsky Institute of Chemical Kinetics and Combustion SB RAS, 3, Institutskaya Str., 630090, Russian Federation; and Novosibirsk State University, 2, Pirogova Str., 630090 Novosibirsk, Russian Federation
Peter S. Sherin: International Tomography Center SB RAS, 3a, Institutskaya Str., 630090 Novosibirsk, Russian Federation; and Novosibirsk State University, 2, Pirogova Str., 630090 Novosibirsk, Russian Federation

sponding fractions are approximately 19–20% and 0.28, while for cyclic alkanes they are lower at 16–17% and 0.22, respectively.

Keywords: diphenylacetylene; exciplex luminescence; magnetic field effect; radical ion pair; spin correlation; X-ray irradiation.

Dedicated to: Kev Salikhov on the occasion of his 80th birthday.

1 Introduction

Paramagnetic intermediates are key participants in diverse chemical processes and determine the direction and depth that they proceed [1]. Often they are the "witnesses" of the occurring events, such as radiation of photo-induced damage to a material, or are introduced deliberately as labels or probes that provide important information on their local environment in a solid matrix [2, 3], on the type and magnitude of molecular mobility in a condensed matter [4–7], on the degree of oxygenation and acidity in biological systems [8, 9], on specific for electron spins interactions that determine the suitability of a material for application in the devices of modern molecular electronics [10–13], etc. The most direct experimental methods to study the radicals are certainly the various implementations of ESR, which has recently enjoyed an explosive experimental and methodological development similar to the earlier proliferation of pulsed NMR.

In those cases when radical concentrations are too low and do not reach the sensitivity threshold of conventional ESR with detection of microwave absorption the methods of indirect ESR detection can be called for [14–17]. Here spins are also manipulated with static and microwave magnetic fields, but detected is not directly MW absorption, but some product of a spin-dependent reaction in a correlated radical pair or more complex system of electron spins, such as luminescence or the yield of cage recombination products. By accumulating the result of reaction in a stable product or converting the act of recombination in the emission of an optical photon, such methods attain exceptional sensitivities for concentrations of transient radicals. On the other hand, they had posed a very important question on the role of spin correlation in chemical reactivity, which resulted in the establishment of a new field of chemical physics, the so-called spin chemistry [18]. The methods of spin chemistry have significantly broadened our knowledge on the mechanisms of important reactions including electron transfer and bond cleavage, as well as on the structure and properties of short-lived radicals and radical ions, and have, e.g. much helped in establishing the mechanism of photosynthesis and the structure of photosynthetic reaction center

[19–22]. The systems of spin chemistry are today used to study the problems of teleportation of a quantum state [23] and of quantum measurement [24–27], the well established ideas and results of spin chemistry, although slowly, but are finding their way into the field of modern functional materials, molecular electronics and spintronics [10–13].

While the methods of spin chemistry provide a tremendous boost in sensitivity to low concentrations of the studied radicals, they also bring their specific complications related to signal formation by not just one, but at least a pair of correlated spins. Thus, for example, for contact radical pairs forming upon photolysis of systems like aromatic ketones and observed by polarized NMR spectra of their recombination products (CIDNP) [28], and for contact radical ion pairs forming upon photoinduced electron transfer to produce equilibrated exciplex and solvent-separated pair and detected by exciplex luminescence [29], it is necessary to correctly take into account a substantial exchange interaction between pair partners and its spatial dependence.

The effects of inter-radical interaction in contact pairs are nearly eliminated in radiation spin chemistry, when radical ion pairs are generated by ionizing irradiation of a nonpolar solution of suitable electron acceptors and donors, with detecting the intensity of recombination luminescence as a function of applied static and/or resonant MW magnetic field [30, 31]. In this case the initial partner separation in the pair is tens of angstroms, while back electron transfer – the recombination – occurs at a distance of about 10 angstroms, and thus the two radical ions of the pair, apart from the obvious coulomb attraction, can be considered independent and linked only by the initial spin correlation imposed upon pair generation at the moment of ionization of a solvent molecule. For this reason radiation chemical systems have served as a proving ground for many theoretical and experimental approaches of spin chemistry, including time-resolved magnetic field effects and quantum beats [32, 33], optically detected ESR [16, 17], level-crossing (MARY) spectroscopy [34], etc. These techniques certainly have their photoinduced counterparts, but these are too abundant to be discussed here.

However, in radiation spin chemistry as well the gain in the simplicity of describing the spin evolution of radical ion pair has to be paid for by certain experimental complications. Radiation generation produces the pairs not as isolated entities, but rather as the so-called spurs, which for the X-irradiation with upper energy cutoff of 40 keV used in this work are about 100 angstroms in diameter and contain about 5–6 overlapping pairs [35–37]. The rapid cross-recombination of the primary pairs electron/solvent radical cations in the spurs within picoseconds leaves the last remaining pair that is not necessarily geminate, i.e. from partners coming from the same parent molecule, and thus not necessarily

spin-correlated. Since all methods of spin chemistry usually rely on the initial spin correlation in the pair, this leads to a substantial drop in the magnitudes of the experimentally observed effects and to introduction of an empirical parameter in the theoretical description, the fraction of spin-correlated pairs θ, that in the conditions of X-irradiation normally falls in the range 0.1–0.4. Several experimental approaches have been proposed to determine θ and are discussed later, but all of them are rather complex and can be applied to a limited range of systems, therefore an extension in the set of tools to determine θ would be most welcome.

Furthermore, radiation generation of the pairs with detection of recombination luminescence is accompanied by a host of background processes that also produce emission of the luminophore present in the solution, which is not related to spin correlation in the pair. An example would be direct energy transfer from an excited solvent molecule to a luminophore molecule, which produces the same emission as recombination of the spin-correlated pair comprising radical ion of the luminophore. Therefore the fraction of magnetosensitive emission in the total intensity of sample luminescence is relatively low and usually is much lower than the maximum possible value determined by the fraction of spin-correlated pairs, being at best several percent in a CW experiment. Moreover, as all emission usually occurs in the same spectral band, it is practically impossible to separate magnetosensitive luminescence related to spin evolution of spin-correlated pairs from background emission by spectral methods in a CW experiment. This is in principle possible in time-resolved experiments, since temporal behavior of the kinetics of recombination luminescence for different channels of its generation may be different, but this would require a complete first-principles modeling of the experimental kinetics, which is at present not feasible due to the complexity of the reaction scheme of radiation chemical processes and the necessity in a large number of poorly known parameters for its specification [38, 39].

In this work we suggest a simple experimental approach to substantially increase the sensitivity of CW methods of radiation spin chemistry with detection of recombination luminescence due to spectral shift of the recombination luminescence in a separate emission band and its selective detection, and apply it to experimentally estimate the fraction of spin-correlated radical ion pairs in X-irradiated alkane solutions. The approach relies on the recently found efficient exciplex formation upon recombination of radiation-induced radical ion pairs [40, 41]: since at the moment of recombination the two radical ions are relatively close, after the back electron transfer to yield an electronically excited molecule the second partner of the pair happens to be next to it, which creates optimal conditions for exciplex generation. As discussed in the previous works [40, 41], the recombination exciplexes can arise from

practically arbitrary donor-acceptor pairs that energetically and sterically allow this, and produce a new longer wavelength band in the emission spectrum. The difference of this radiation generation of exciplexes in comparison with well-studied photochemical and electrochemical methods is in the arbitrary short lifetime of the excited state generated upon recombination, as the precursor pair for the exciplex is formed nearly at contact and the diffusion-controlled bulk quenching reaction needed for optical generation [42–50] is not required, and quite relaxed requirements to radical ion stability germane for electrochemical generation of exciplexes from radical ions injected from electrodes or chemically [51–53], since radiation-induced pairs recombine in tens of nanoseconds.

Experimentally convenient pairs to study the recombination exciplexes turned out to be pairs *N,N*-dimethylaniline (DMA) – aromatic electron acceptor, which produce emission spectra containing the bands of intrinsic emission of DMA and the acceptor, as well as a red-shifted emission band of exciplex (DMA-acceptor)*. Especially convenient is the pair DMA – diphenylacetylene (tolane, **T**) [40], since the very short lifetime of intrinsic emission of **T** (8 ps [54, 55]) for sure eliminates exciplex generation *via* bulk reaction of its excited molecule with a DMA molecule, so the exciplexes form exclusively *via* the recombination channel, while its very low quantum yield of intrinsic luminescence (0.00336 [56]) simplifies the spectrum or recombination luminescence, leaving only the bands of intrinsic DMA emission and exciplex emission.

Furthermore, as the exciplex emission in this pair is generated only *via* the pair recombination, its intensity is magnetosensitive with the magnitude of magnetic field effect of up to 20%, reaching the upper limit set by the fraction of spin-correlated pairs. Since recombination of the radical ion pair in these conditions is irreversible, all magnetosensitivity of the exciplex emission is completely inherited from spin evolution in the radiation-induced radical ion pair, while the sole effect of exciplex formation is simply a transfer of the recombination luminescence in the exciplex emission band, which separates it from other, background processes of excited state generation. Therefore the magnetosensitivity of emission of radiation-induced exciplexes in alkanes is principally different from the magnetosensitivity of emission of photoinduced exciplexes in moderately polar solvents that is due to reversible transitions between exciplexes and solvent-separated radical ion pairs [29, 57–63].

The only inconvenience of the DMA – diphenylacetylene pair in this context is a rather substantial overlap of the emission bands of DMA and exciplex, which requires spectrum decomposition into individual components before analyzing the magnetic field effect. However, electronic (and steric) properties of donor-acceptor systems can be adjusted by introducing donor or acceptor substituents

in the parent molecules [57, 64, 65]. While for most classic donor-acceptor systems (naphthalene – DMA, anthracene – DMA, pyrene – DMA) synthesizing a broad range of substituted electron acceptors is a rather daunting task, as for them there is no single and straightforward reaction of aromatic substitution and each target substituted molecule would require a dedicated synthetic procedure, almost any substituted diphenylacetylenes can be readily prepared by Sonogashira or Castro cross-coupling [66, 67] from the corresponding arylhalogenide and either terminal acetylene or acetylenide.

In this work we suggest a more convenient probe exciplex system for studies in radiation spin chemistry. To this end using the Sonogashira reaction we synthesized a novel acceptor-substituted diphenylacetylene, 1-(phenylethynyl)-4-(trifluoromethyl)benzene (*p*-trifluorotolane, CF_3-tolane, **FT**), which retains all useful in this context properties of diphenylacetylene (a very short lifetime and rather low quantum yield of intrinsic emission, efficient electron capture in alkanes to produce radical anion and efficient exciplex formation upon recombination in pair with DMA radical cation), while exhibiting a shifted to red exciplex emission band as compared to the parent system DMA – diphenylacetylene. After chemical, luminescent, radiation and spin-chemical characterization of the new system we used the magnitude of magnetic field effect in its exciplex emission band for experimental estimation of the fraction of spin-correlated pairs in a representative set of linear, cyclic and branched alkanes.

2 Materials and methods

2.1 Experimental

Purified *n*-hexane, *n*-heptane, *n*-octane, *n*-decane, *n*-dodecane, *n*-hexadecane, isooctane, 2,3-dimethylbutane, squalane, cyclohexane, methylcyclohexane were used as the solvents. DMA (99%, Aldrich) prior to experiments was distilled over zinc powder collecting the 193–195 °C fraction. Chromatographic analysis combined with mass-spectrometry showed DMA purity more than 99%, with *N*-methylaniline and *N,N*-dimethyl-*m*-aminoaniline as the major impurities. All experiments were carried out at room temperature without explicit temperature control.

The CW spectra of magnetosensitive recombination luminescence were obtained with a Magnetically Affected Reaction Yield (MARY) spectrometer with spectral resolution of luminescence (an MDR-206 grating monochromator, LOMO Photonics, St. Petersburg, Russia, objective focus length 180 mm, grating 1200 lines·mm^{-1}, inverse linear dispersion 4.3 nm·mm^{-1}, and a FEU-100

PMT for detection) described elsewhere [68]. The samples were irradiated with a BSV-27-Mo X-ray tube (Svetlana, St. Petersburg, Russia), 40 kV, 20 mA, detection monochromator slits 2.2 mm/2.2 mm (spectral resolution about 10 nm). The presented spectra are averages over 8–16 independent wavelength scans of 256 points. Luminescence intensities are given as arbitrary units corresponding to the output signal of detector and are consistent for all spectra. The pairs of spectra in magnetic field (20 mT) and in zero field were recorded simultaneously for each scan by registering at each wavelength point the intensity of emission with applied field and without field before advancing to the next point. The samples for magnetic field effect measurements were 300 μL of degassed solution sealed in a thin-walled round ampoule with O.D. 5 mm made from molybdenum glass, which produces no intrinsic luminescence under X-radiation. The concentration dependence and the oxygen quenching spectra in low-volatile *n*-dodecane were taken in a reusable cuvette with vacuum stopcock instead of individual samples to improve repeatability of sample geometry. Further details on the experimental procedure and the choice of ampoule material can be found elsewhere [68].

Optically detected ESR spectra and modulation optically detected magnetic field effects (MARY spectra) under X-irradiation were recorded in stationary conditions as described in refs. [69, 70], respectively. The sample containing about 1 mL of degassed solution in a quartz cuvette was placed into magnetic field of a Bruker ER-200D CW X-Band ESR spectrometer equipped with an X-ray tube for sample irradiation (Mo, 40 kV, 20 mA), a pair of coils with a separate current source to provide constant "negative" shift of the field (for MARY experiments), and a PMT for fluorescence detection. All integral emission without spectral shaping was detected. The scanned magnetic field was modulated at a frequency of 12.5 kHz with an amplitude of up to 0.5 mT. A Stanford SR-810 Lock-In Amplifier and computer averaging over four scans were used to get the spectra as the first derivatives of the actual field dependencies. Microwave power for OD ESR experiments was 0.8 W. MARY experiments were carried out without microwave pumping.

The discussed radiation-induced luminescence kinetics were obtained on a home-built nanosecond pulse fluorometer [71]. The luminescence is generated by short – about 1.5–3 ns – X-ray pulses generated by hitting a molybdenum target by a bunch of electrons with the energy of 30–40 keV. The full intensity of recombination luminescence without spectral selection is detected in this experiment using time-correlated single photon counting. The magnetic field at the sample can be controlled in the range of 0–1.9 T, 0.1 T was used in this work. A more detailed description of the experimental procedure for X-ray induced time-resolved experiment can be found elsewhere [72].

The luminescent properties of the synthesized 1-(phenylethynyl)-4-(trifluoromethyl)benzene under optical excitation were characterized on a commercial Edinburgh Instruments FLSP-920 spectrofluorometer (Great Britain). CW emission and excitation spectra were recorded using a wide-band Xenon lamp (OSRAM XBO, 450W, Germany), slit widths for excitation and detection monochromators 2.5 mm. Time-resolved fluorescence decay profiles were taken using an EPLED-270 diode, excitation wavelength 275 nm, full width at the half maximum 0.8 ns, with spectral resolution of the detection monochromator 20 nm. Kinetics of fluorescence decay were analyzed using a numerical convolution of the instrument function with an exponential function. Optical absorption spectra were recorded using a Shimadzu UV-2401PC (Japan) and an Agilent HP8453 (USA) spectrometers.

2.2 Synthesis of 1-(phenylethynyl)-4-(trifluoromethyl)benzene

The target 1-(phenylethynyl)-4-(trifluoromethyl)benzene was prepared by Sonogashira cross-coupling [66] of phenylacetylene and 1-bromo-4-(trifluoromethyl) benzene as shown in Scheme 1.

Reagent weights were calculated for $2{\cdot}10^{-3}$ mol of the starting bromide with 10% molar excess of the terminal acetylene in 10 mL of toluene. The reaction was catalyzed by 5 mg $[Pd(PPh_3)_2Cl_2]$, with 5 mg CuI and 1 mL triethylamine (3× molar excess) added to the mixture, which was stirred in the argon atmosphere for 1 h at 70°C. After completion of the reaction (control by TLC, Merck Silica gel 60 F_{254} plates) the produced toluene solution was passed through a column with SiO_2 using toluene as the eluent and evaporated *in vacuo*.

The obtained residue was dissolved in *n*-hexane and passed through a column with SiO_2, using *n*-hexane as the eluent and monitoring product separation with TLC. The eluate of 1-(phenylethynyl)-4-(trifluoromethyl)benzene was evaporated *in vacuo* and recrystallized twice from *n*-hexane. The obtained compound is a white crystalline powder with mp 102–104 °C (lit. 100 °C), IR: 1107; 1323; 1608; 2220 cm^{-1}; ^1H NMR (400 MHz, $CDCl_3$): 7.33–7.37 (m, 3H); 7.51–7.54 (m, 2H); 7.60 (dd, 4H). The obtained analytical results agree with published data [73], the raw ^1H NMR and FTIR spectra are given in Supporting Information.

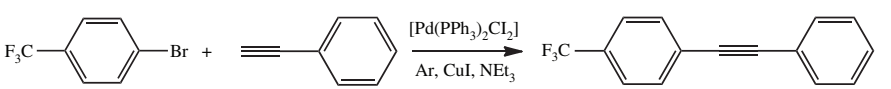

Scheme 1: Synthesis of 1-(phenylethynyl)-4-(trifluoromethyl)benzene by Sonogashira cross-coupling [66].

3 Results and discussion

3.1 Optical and luminescent properties of 1-(phenylethynyl)-4-(trifluoromethyl)benzene

Figure 1 shows optical absorption spectra of the synthesized compound **FT** in alkane in comparison with unsubstituted diphenylacetylene **T**. As can be seen, introduction of the -CF_3 substituent in the *para*-position of diphenylacetylene does not change the shape of the absorption spectrum and only leads to its red shift of about 5 nm. This is rather typical of *para*-substituted diphenylacetylenes with compact substituents that do not extend π-system and significantly lower its symmetry [74, 75].

As demonstrated elsewhere [76], the luminescent properties of *para*-substituted diphenylacetylenes are also rather close to unsubstitited tolane. Thus, 1-metoxy-4-(phenylethynyl)benzene, similar to **T**, emits from its second singlet excited state having lifetime of 7 ps [74, 75, 77]. Transition $S_1 \rightarrow S_0$ in this molecule is also forbidden, and still S_1 lifetime is very short at 270 ps, as determined in ref. [76].

Figure 2 shows spectra of luminescence and excitation and luminescence decay profile for solution of **FT** in acetonitrile. Luminescence quantum yield determined by procedure described in ref. [78], taking solution of **T** in ethyl alcohol as the reference with a known and similar quantum yield (0.00336 at room temperature [56]), was found to be 0.010 ± 0.001 at room temperature. The estimated from fitting upper bound for lifetime of **FT** excited state is about 200 ps, which is attainable time resolution for the used excitation diode, and most probably corresponds to forbidden $S_1 \rightarrow S_0$ transition, as in unsubstituted **T** [74,

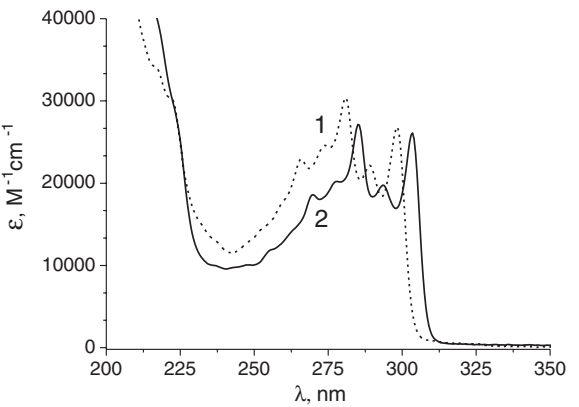

Fig. 1: Optical absorption spectra for solutions of **T** (**1**) and **FT** (**2**) in *n*-dodecane.

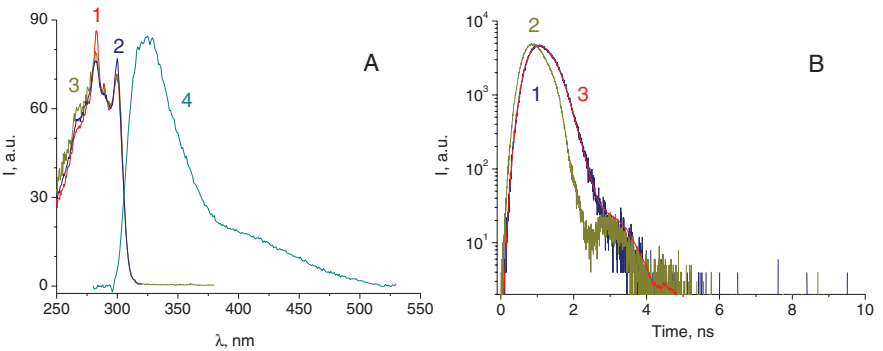

Fig. 2: (A) Normalized for equal emission intensity for excitation at 287 nm excitation spectra of **FT** acetonitrile with detection at 310 nm (**1**), 330 nm (**2**) and 450 nm (**3**). Normalized luminescence spectrum of **FT** in acetonitrile (**4**), excitation at 275 nm, spectral resolution 2.5 nm, **FT** concentration $6 \cdot 10^{-6}$ M. (B) Luminescence decay profile of **FT** in acetonitrile, excitation at 275 nm and detection at 330 nm (**1**), and instrument function of the excitation source (**2**). Spectral resolution 20 nm, **FT** concentration $6 \cdot 10^{-6}$ M. Curve **3** shows fitting of the luminescence decay profile by an exponential function with characteristic time 211 ps. Similar to unsubstituted diphenylacetylene, the time provided by such fitting is most probably attributable to the slower forbidden transition $S_1 \rightarrow S_0$, with no observable traces of the faster allowed transition $S_2 \rightarrow S_0$, while bimodal shape of the spectrum corresponds to both transitions $S_1 \rightarrow S_0$ and $S_2 \rightarrow S_0$ [74, 76].

75, 77]. The shorter-living S_2 state was not resolved in the luminescence decay profiles. Thus, the synthesized *para*-CF_3-substituted diphenylacetylene has luminescent properties similar to unsubstituted tolane, exhibiting very short lifetimes of excited states (both S_2 and S_1) and low but finite luminescence quantum yield. As demonstrated below, in CW experiments under X-irradiation **FT** produces practically no intrinsic luminescence in comparison with emission in the bands of the second partner (DMA) and exciplex, while in time-resolved experiments with single photon counting its quantum yield, being a factor of three higher than for **T**, turns out to be sufficient to produce kinetics of recombination luminescence at nanosecond time scale for comfortably low concentrations of about 10^{-3} M.

3.2 Exciplex formation in the pair 1-(phenylethynyl)-4-(trifluoromethyl)benzene – DMA *via* radical ion pair recombination

Figure 3A shows the spectra of radiation-generated luminescence for mixtures of 1-(phenylethynyl)-4-(trifluoromethyl)benzene and DMA in *n*-dodecane for varied concentrations of the electron acceptor. The major components of the spectra are exciplex emission (long-wavelength band) that dominates as **FT** concentration is

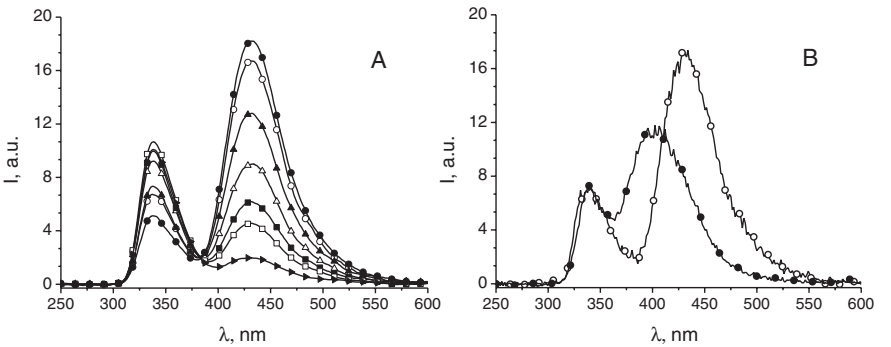

Fig. 3: (A) Averaged spectra of X-ray generated luminescence for mixtures of 1-(phenylethynyl)-4-(trifluoromethyl)benzene and DMA in *n*-dodecane. Concentration of DMA $1{\cdot}10^{-2}$ M in all spectra; **FT:** ● – $1{\cdot}10^{-2}$ M, ○ – $6{\cdot}10^{-3}$ M, ▲ – $4{\cdot}10^{-3}$ M, △ – $2{\cdot}10^{-3}$ M, ■ – $1{\cdot}10^{-3}$ M, □ – $6{\cdot}10^{-4}$ M, ▶ – $2{\cdot}10^{-4}$ M. (B) Spectra of X-ray generated luminescence for mixtures of: ● – $6{\cdot}10^{-3}$ M **T**, $1{\cdot}10^{-2}$ M DMA; ○ – $6{\cdot}10^{-3}$ M **FT**, $1{\cdot}10^{-2}$ M DMA in *n*-dodecane.

increased and intrinsic emission of DMA (short-wavelength band), which is itself a satisfactory luminophore (quantum yield 0.11, fluorescence lifetime 2.4 ns [79]) and whose excited states are mostly generated by direct energy transfer from generously forming excited states of solvent molecules (*n*-dodecane quantum yield 0.0055 [80], fluorescence lifetime 4.2 ns [81]). Figure 3B shows taken in identical conditions spectra of radiation-generated luminescence for mixtures of **T** or **FT** and DMA in *n*-dodecane. It can be seen that the introduced acceptor substituent did not hinder exciplex formation and shifted exciplex emission band to the red by about 35 nm, significantly improving band separation in the spectrum as compared to unsubstituted diphenylacetylene.

Using the earlier suggested approach for estimation of lifetimes of radiation-induced exciplexes [82], the lifetime of 1-(phenylethynyl)-4-(trifluoromethyl) benzene – DMA exciplex in *n*-dodecane at room temperature was estimated as 61 ± 3 ns, which is somewhat higher than 49 ± 2 ns for tolane – DMA exciplex [82]. The lifetime was estimated from the degree of relative quenching of exciplex emission with dissolved oxygen in comparison to quenching of a reference luminophore with similar excited state lifetime in identical conditions. Typical spectra of radiation-generated luminescence for a degassed sample and the same sample equilibrated with normal atmosphere are shown in Figure 4A. Figure 4B shows the reconstructed exciplex emission spectrum for this system obtained by subtracting the spectra from Figure 4A normalized to the maxima of the short-wavelength band as suggested by the Reviewer to paper [82].

The area under a spectrum band is a standard measure of the number of species contributing to the band, and thus the area under the exciplex emission

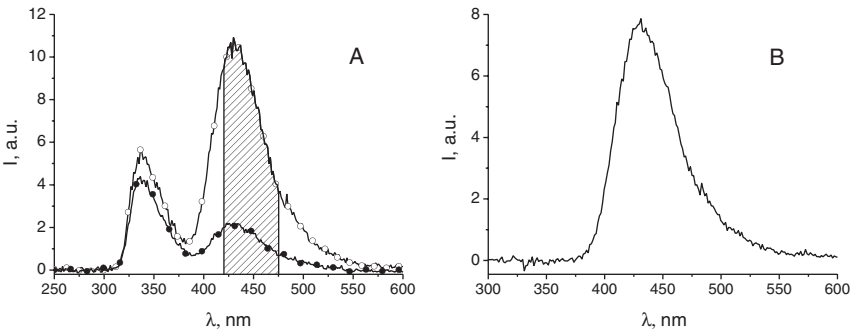

Fig. 4: (A) X-ray generated luminescence spectra of degassed (○) and equilibrated with normal atmosphere (●) mixtures of $6{\cdot}10^{-3}$ M **FT**, $1{\cdot}10^{-2}$ M DMA in *n*-dodecane. The integral quenching of the exciplex emission band $I_0/I - 1$ in the indicated wavelength range is 3.7 ± 0.2. (B) Emission spectrum of 1-(phenylethynyl)-4-(trifluoromethyl)benzene – DMA exciplex obtained from emission spectra of the same sample solution of $6{\cdot}10^{-3}$ M **FT** and $1{\cdot}10^{-2}$ M DMA recorded in the presence and absence of dissolved oxygen (see ref. [82] for details).

band can be used to study the amount of generated exciplexes as a function of experimental parameters, such as sample composition. For the 1-(phenylethynyl)-4-(trifluoromethyl)benzene – DMA exciplex in *n*-dodecane integration can be performed in the range 415–475 nm, in which emission comes exclusively from the exciplex and contains no contribution from intrinsic DMA luminescence. Baseline correction is performed by averaging over the initial part of the spectrum containing no emission and subtracting the average value from the spectrum. Figure 5A shows thus obtained areas vs. **FT** concentration for the spectra

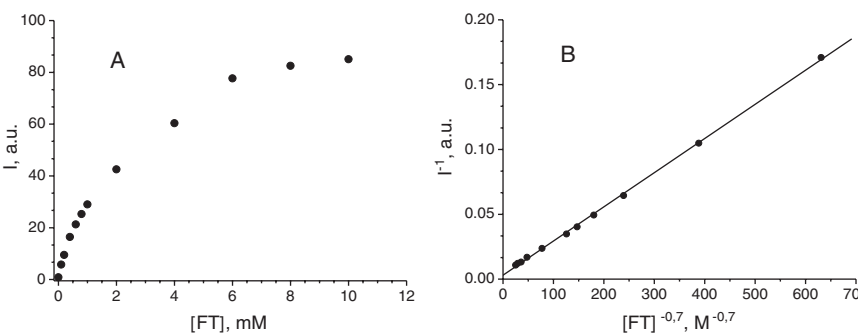

Fig. 5: (A) Area under the exciplex emission band in the range 415–475 nm vs. **FT** concentration in the system 1-(phenylethynyl)-4-(trifluoromethyl)benzene – DMA in *n*-dodecane. (B) Linearization of the dependence of Figure 5A in indicated coordinates, shown linear fit is $I^{-1} = 0.0031 + 2.6{\cdot}10^{-4}/[\mathbf{FT}]^{0.7}$, $\alpha = 34.5$, see expression (3).

of radiation-generated luminescence from Figure 3A, which can be used to verify the origin of the detected exciplex emission.

The characteristic shape of the obtained dependence is similar to concentration dependence of the intensity of luminescence for hexafluorobenzene (HFB) solutions irradiated with β-particles reported in ref [83]. In this case the intensity of HFB luminescence is determined by the efficiency of electron capture in the primary radical ion pair by HFB according to reaction (1) below. The subsequent recombination of the forming secondary radical ion pair *via* reaction (2), where $S^{+\bullet}$ is solvent radical cation, produces an excited HFB molecule that emits the detected luminescence.

$$e^- + HFB \rightarrow HFB^{-\bullet} \quad (1)$$

$$S^{+\bullet} + HFB^{-\bullet} \rightarrow HFB^* + S \quad (2)$$

To detect only the recombination luminescence the authors of ref. [83] used alkanes with very low intrinsic quantum yield of fluorescence φ_f, such as isooctane ($\varphi_f < 10^{-5}$ [80]). As was earlier experimentally demonstrated in refs. [84, 85], the probability of electron capture by an acceptor molecule in the case of detecting luminescence of the acceptor is given by the following expression:

$$p^{\dagger} = \frac{(\alpha C)^{0.7}}{1 + (\alpha C)^{0.7}} \quad (3)$$

where $p^{\dagger}$ is the probability of quenching the primary radical ion pair $S^{+\bullet}/e^-$, which is equal to the probability of electron capture by HFB in reaction (1), α is a quenching parameter that depends on the particular solvent – acceptor system and does not depend on acceptor concentration, C is HFB concentration in the mixture. A similar expression was also obtained for the dependence of radiation yield of alkyl radicals on the concentrations of alkylhalide electron acceptors/quenchers, such as CH_3Br, in cyclohexane [86].

Within the context of the cited works, if all the observed excited species in solution are generated only as a result of radical ion pair recombination *via* reaction (2), the experimentally registered luminescence intensity should be proportional to $p^{\dagger}$. As a result, the reciprocal of the intensity of HFB luminescence should be a linear function of $C^{-0.7}$ where C is HFB concentration in the mixture, while the ratio of the y-axis cutoff and the slope for the obtained linear function produces the unknown parameter α that can be independently estimated theoretically [83, 84].

As Figure 5B demonstrates, in the described coordinates the concentration dependence of integral exciplex emission from Figure 5a is also linear in the range of **FT** concentration 10^{-4}–10^{-2} M. This confirms that in the system under study the

exciplexes are indeed formed only *via* recombination of the secondary radical ion pair $D^{+\bullet}/A^{-\bullet}$, where D is DMA and A is 1-(phenylethynyl)-4-(trifluoromethyl) benzene. It should also be stressed that, as opposed to the cited concentration dependence for HFB, in the system 1-(phenylethynyl)-4-(trifluoromethyl)benzene – DMA there is no need in non-luminescing solvents, in which the excited states are produced only upon recombination of radical ion pairs, as recombination formation of exciplexes with emission shifted to the red relative to the intrinsic emission of the mixture components automatically separates the recombination luminescence and helps get rid of non-recombination contributions to the observed emission.

3.3 OD ESR and MARY spectra of the probe pair

Figure 6 shows typical results of CW radiation spin chemistry experiments, i.e. Optically Detected ESR (OD ESR) and Magnetically Affected Reaction Yield (MARY) spectra, for the mixtures of **FT** and DMA in *n*-dodecane. OD ESR provides combined spectra of the short lived radical anion and radical cation that recombine to produce detectable luminescence as a single trace that is approximately the superposition of the independent spectra for the two partners [16, 17], apart from the finer spectral shape details due to interlinked spin relaxation of the two radical ions [87, 88] and, on very rare occasions, certain coherent features specific

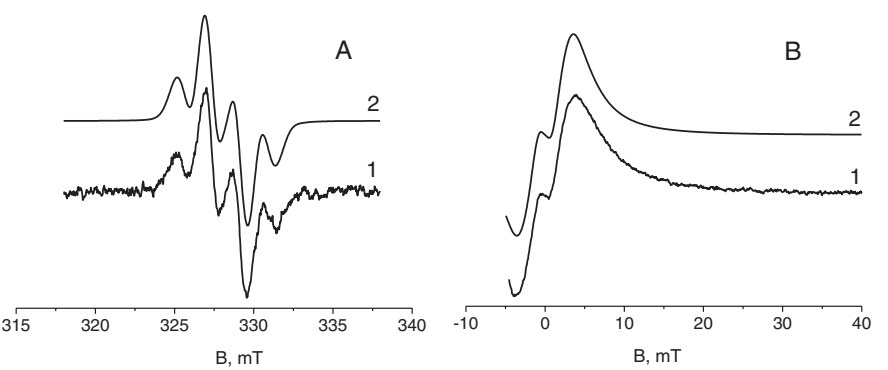

Fig. 6: (A) OD ESR spectrum for a mixture of $1{\cdot}10^{-2}$ M **FT** and $1{\cdot}10^{-2}$ M DMA in *n*-dodecane: **1** – experimental spectrum taken with modulation amplitude 0.2 mT at 12.5 kHz, MW power 800 mW, **2** – its simulation (see text for details). (B) MARY spectrum for the same mixture of $1{\cdot}10^{-2}$ M **FT** and $1{\cdot}10^{-2}$ M DMA in *n*-dodecane: **1** – experimental spectrum taken with modulation amplitude 0.5 mT at 12.5 kHz, **2** – its simulation (see text for details).

for spin-correlated pairs [89–91] or partial spectral inversion at high MW power due to spin-locking [92, 93], as well as consecutive pairs [94, 95]. When applied to exciplex-forming systems as discussed in this work, the registered OD ESR spectrum can be used to identify the recombining pair from the characteristic hyperfine couplings of the two radical ions, with the possibility to detect all integral luminescence from the sample without spectral limiting in the case of dominating exciplex emission.

Figure 6A shows an OD ESR spectrum for a mixture of 1-(phenylethynyl)-4-(trifluoromethyl)benzene and DMA in *n*-dodecane. The presence of a -CF_3 substituent in diphenylacetylene significantly improves the identification capability of this approach, as fluorines usually have rather substantial hyperfine coupling (HFC) constants [96], while several equivalent nuclei with the dominant HFC produce a very characteristic ESR spectrum. Thus, a quartet from three equivalent spin ½ nuclei is immediately recognizable in the spectrum shown in Figure 6a. The accompanying simulation was obtained using WinSim package [97]. DMA radical cation was modeled with a fixed set of HFC constants that were estimated in DFT calculations in ref. [98]: 1.30 mT (6H), –0.72 mT (1N), 0.83 mT (1H), –0.43 mT (2H), 0.09 mT (2H) with a homogeneous width at half magnitude of 0.41 mT. Radical anion of 1-(phenylethynyl)-4-(trifluoromethyl)benzene for this spectrum was modeled as three equivalent fluorines with (hitherto unknown) HFC constant of 1.67 mT and inhomogeneous peak-to-peak width of 0.58 mT. An additional species with an unresolved spectrum having a homogeneous width at half magnitude of 0.57 mT was also introduced in the simulation, which corresponds to exchange-narrowed in its parent matrix radical cation of *n*-dodecane, the precursor to $DMA^{+\bullet}$.

We note that the shown spectrum taken at **FT** concentration of 10^{-2} M already corresponds to the region of intermediate exchange [99] (mean residence time at the diffusion-controlled rate constant of about 10^{10} $M^{-1}s^{-1}$ is about 10 ns and is comparable to the inverse ESR spectrum width of the radical anion in frequency units), and upon reducing the concentration of **FT** down to 10^{-3} M to suppress the degenerate electron exchange between $\mathbf{FT}^{-\bullet}$ and neutral **FT** molecules the spectrum is modeled with slightly higher HFC for the three fluorines of about 1.87 mT, which are closer to the intrinsic HFC values. However, even for such inconvenient for quantitative interpretation concentrations the spectrum has a very characteristic shape and unequivocally identifies the radical anion of the recombining pair.

The recombining radical ion pair can also be identified by its MARY spectrum that is the first derivative of the magnetic field dependence of the intensity of recombination luminescence in the vicinity of zero field without MW pumping applied [34]. In this case the shape of the recorded spectrum is determined by the second moments of the ESR spectra of the pair partners and their relative

magnitudes (close values or dominating hyperfine interactions in one of the pair partners), as well as lifetimes and relaxation times of the recombining spin-correlated radical ion pair [100].

Figure 6B shows an experimental MARY spectrum for the same sample used for Figure 6A and its modeling that was performed in the model of equivalent nuclei [101] which account for the required second moment of the ESR spectrum, with power-law recombination kinetics $\alpha/2(1+\alpha t)^{3/2}$ approximated as a set of five exponentials [102]. HFC in the radical anion of **FT** was modeled as three equivalent spin ½ nuclei with HFC constant 1.67 mT, HFC of DMA radical cation was approximated as a set of 10 equivalent spin ½ nuclei with HFC constant 1.1 mT, which provides the required second moment of the ESR spectrum of $DMA^{+\bullet}$. Relaxation times T_2 for both partners were set at 11 ns to account for the process of degenerate charge exchange in both radical ions having concentration of their parent molecules of $1{\cdot}10^{-2}$ M, which in MARY spectra reveals itself as phase relaxation [100, 103, 104].

The general look of the MARY spectrum with a broad featureless background of magnetic field effect and not very prominent zero field line is rather typical for a pair with substantial and evenly distributed between partners hyperfine couplings. Although for systems with simple hyperfine structure the spectrum could have had additional lines in magnetic fields that are multiples of the HFC constant [101, 105–114], and three equivalent nuclei could have produced a specific line at 15/4 of the coupling constant, as demonstrated earlier for radical anion of 1,3,5-trifluorobenzene [113], the substantial couplings in the other partner, rather low value of the HFC constant for the three fluorines, and short relaxation times together wipe away any resolved structure. It can also be seen that the model curve at the wings is decaying somewhat faster than the experimental spectrum. This is due to modeling the HFC of $DMA^{+\bullet}$ as a set of equivalent spin ½ nuclei giving a Gaussian contour, a situation for which a closed analytical solution is available [101, 106], while the actual ESR spectrum of $DMA^{+\bullet}$ noticeably departs from Gaussian due to the presence of a spin 1 nucleus (N). The importance of explicitly accounting for higher-spin nuclei to accurately reproduce the wings of MARY spectra was earlier demonstrated for pairs comprising radical anions of quinolinate complexes of metal cations with nuclear spins 3/2–5/2 that bear the dominant HFC [115]. Another available model to describe spin evolution in MARY spectra, the semiclassical description [70, 116–118], also represents the HFC as a Gaussian contour and thus does not mend the situation with DMA radical cation, while an explicit description of the hyperfine structure in low magnetic fields, although undertaken several times for selected systems [103, 116, 119], drastically complicates description without providing any new insight for the purpose of this work, and therefore was not attempted.

We also note that the presented OD ESR and MARY spectra have about an order of magnitude better signal-to-noise ratio in comparison to spectra taken in identical conditions for systems with similar intrinsic luminescence properties that do not form exciplexes, which is a direct consequence of generating a new high-intensity exciplex emission band that comprises all the magnetosensitive recombination luminescence that for the discussed probe pair is the dominant emission band.

3.4 Time-resolved magnetic field effect for a pair comprising FT radical anion

Luminescent properties of **FT** allow directly observing temporal spin state evolution of spin-correlated radical ion pairs comprising its radical anion to characterize the radical anion itself and to determine the fraction of spin-correlated pairs among all pairs that recombine at the nanosecond time scale using the method of Time-Resolved Magnetic Field Effect (TR MFE) [120, 121]. To this end we measured the kinetics of recombination fluorescence decay for solutions of $2{\cdot}10^{-3}$ M **FT** in *n*-dodecane and cyclohexane in zero field and in the applied field of B = 0.1 T. The second partner of the probe pair, DMA, in these experiments was not introduced into the system, since then unavoidable formation of the recombination exciplex with a long emission lifetime would render impossible observation of any resolved quantum beats. On the other hand, the very short intrinsic emission lifetime of **FT** provides for excellent quantum beats in the pair with solvent radical cation $S^{+\bullet}$/$\mathbf{FT}^{-\bullet}$. This is demonstrated in Figure 7 that shows the result of dividing the kinetics obtained in applied field 0.1 T by the corresponding kinetics in zero field, i.e. the TR MFE curves.

Acceptor concentration, $2{\cdot}10^{-3}$ M, was chosen to rapidly, in a fraction of nanosecond, capture the excess electrons in *n*-dodecane by **FT** (typical rate constant is about $2{\cdot}10^{11}$ $M^{-1}{\cdot}s^{-1}$ [122]), while having the characteristic time of encounters 50–100 ns for species with molecular mobility, thus ensuring that the counter ion for $\mathbf{FT}^{-\bullet}$ is solvent radical cation $S^{+\bullet}$. ESR spectrum of the latter is narrowed due to degenerate electron exchange with parent solvent molecules [123], therefore its contribution to the observed beats is not so pronounced. In cyclohexane solution electron capture proceeds even faster, but due to faster solvent hole mobility in a cyclic alkane [124–126] radical cation capture by **FT** is also possible, which explains the larger width of the counter-ion that was introduced in modeling the cyclohexane TR MFE curve in Figure 7B as compared to the *n*-dodecane curve of Figure 7A.

The most revealing feature of the presented TR MFE curves is a pronounced dip at approximately 18 ns, which is very typical for quantum beats in radical ion

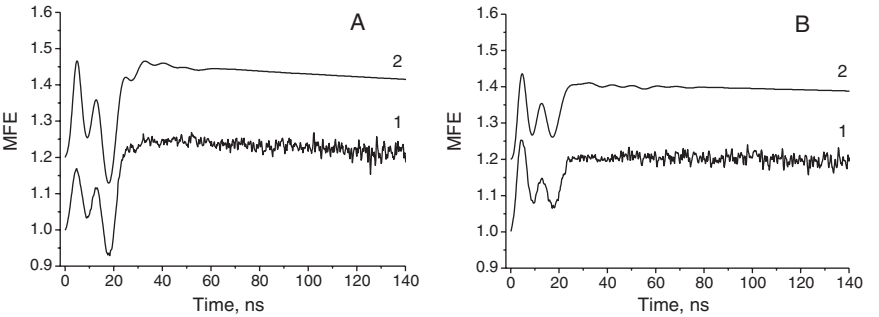

Fig. 7: (A) Experimental (**1**) and calculated (**2**, shifted upwards by 0.2) TR MFE curves for solution of $2 \cdot 10^{-3}$ M **FT** in *n*-dodecane. Modeling parameters: A(3F) = 1.93 mT ($\mathbf{FT}^{-}$), $\Delta = 0.15$ mT (S^{+}), $T_1 = 650$ ns, $T_2 = 16$ ns, $\theta = 0.28$. Temperature 298 K, $B_0 = 0.1$ T. (B) Experimental (**1**) and calculated (**2**, shifted upwards by 0.2) TR MFE curves for solution of $2 \cdot 10^{-3}$ M **FT** in cyclohexane. Modeling parameters: A(3F) = 1.93 mT ($\mathbf{FT}^{-}$), $\Delta = 0.35$ mT (S^{+}), $T_1 = 1200$ ns, $T_2 = 19$ ns, $\theta = 0.22$. Temperature 298 K, $B_0 = 0.1$ T.

pairs comprising partners, in which the unpaired electron interacts with an odd number of equivalent nuclei in one partner and the ESR spectrum width of the second partner is much less than of the first one [127]. Modeling demonstrates that the shown case indeed requires three equivalent spin ½ nuclei with HFC about 1.93 mT that have to be attributed to the radical anion of **FT**. A certain discrepancy between peak amplitudes in the experimental and simulated curves at early times is explained by a contribution of direct energy transfer from excited solvent molecules to luminophore, as the corresponding luminescence at times of units of nanoseconds is only weakly sensitive to magnetic field and smears the beats at slightly later times. The coupling of about 2 mT provides an optimal match with the time resolution of the experimental setup, allowing to detect several periods of high-quality well-resolved beats, and radical anion of 1-(phenylethynyl)-4-(trifluoromethyl)benzene will be a partner of choice in further quantum beats studies. Earlier available examples of fluorinated radical anions with equivalent nuclei, like hexafluorobenzene radical anion [96], had too high a coupling and thus too fast spin evolution to directly resolve it in a TR MFE experiment.

We finally note that the amplitudes of MFE in *n*-dodecane is somewhat higher than in cyclohexane, and that in both solvents the curves decay with a characteristic time of 600–700 ns, which can be considered as spin-lattice relaxation time for the observed radical ion pair in the conditions of this experiment. The fractions of spin-correlated pairs extracted from modeling of these curves and qualitatively given by the initial heights of the decaying tails of the TR MFE curves, were found to be 0.28 for *n*-dodecane and 0.22 for cyclohexane, these values will

be used in the next section to calibrate the values for the representative set of solvents obtained from the magnetic field effect in the exciplex emission band for the probe pair.

3.5 Magnetic field effect in the exciplex emission band in a set of alkanes

Donor-acceptor pair 1-(phenylethynyl)-4-(trifluoromethyl)benzene – DMA turned out to be a very convenient system to study the magnitude of magnetic field effect in the exciplex emission band, and the fraction of spin-correlated radical ion pairs that is directly linked to it, in various nonpolar solvents. First, as has been demonstrated above, all exciplexes in this system form only as a result of magnetosensitive radical ion pair recombination and do not appear as a result of a sequence of not magnetically sensitive reactions, such as direct energy transfer from an excited solvent molecule to any of the mixture components with subsequent bulk reaction between the formed excited molecule and its partner. Second, exciplex emission band is substantially shifted to the red with respect to intrinsic luminescence of the individual mixture components, with a very low intrinsic quantum yield of the "luminophore" itself, which simplifies a reliable determination of the magnitude of magnetic field effect due to pair recombination without emission spectrum decomposition into separate components.

As an example of the probe application of the **FT** – DMA pair we determined the magnitudes of magnetic field effect in the exciplex emission band (χ_E) in 11 alkanes with different properties that can be divided into three groups. The first group includes *n*-alkanes of varied chain length: C_6, C_7, C_8, C_{10}, C_{12}, C_{16}, for which viscosity, luminescence quantum yield and lifetime of the excited state all increase from C_6 to C_{16} [80, 81, 128]. Of relevance to radiation spin chemistry is also the increasing lifetime of solvent radical cation in neat liquids with increasing chain length [129]. The second group comprises cyclohexane and methylcyclohexane, which feature the so-called "fast solvent hole", i.e. the rate of reaction of the solvent radical cation $S^{+\bullet}$ with an electron donor D to produce $D^{+\bullet}$ is an order of magnitude higher than the diffusion-controlled limit [124–126]. The third group consists of various branched alkanes, including non-luminescing isooctane (2,2,4-trimethylpentane) [80, 128], having high viscosity but fast solvent hole squalane (2,6,10,15,19,23-hexamethyltetracosane) [130, 131] and a typical vicinal alkane 2,3-dimethylbutane with moderate luminescence [80, 128]. Some physico-chemical and luminescent properties of the studied alkanes are listed in Table 1.

For each solvent five independent pairs of spectra of radiation-generated recombination luminescence in applied field 20 mT, sufficient to saturate the hyperfine-induced spin evolution in the probe radical ion pair (*cf.* its MARY spectrum in Figure 6B) and in zero field were experimentally obtained, from which χ_E values were determined and statistically evaluated. Figure 8 shows one pair of typical spectra for four representative solvents across all groups, the spectra for all 11 solvents are given in the Supporting Information. The deviations to χ_E values listed in the figure caption are the confidence interval (P = 0.95) for a given set of experimental spectra.

As above, to improve the signal-to-noise ratio when determining χ_E the exciplex emission bands in the spectra in applied field and in zero field were integrated in wavelength range 415–475 nm that contains only the exciplex emission. The magnitude of the magnetic field effect in the band of intrinsic DMA luminescence χ_{DMA} was similarly determined by integrating in the range 315–360 nm. Thus obtained χ_E and χ_{DMA} values for all 11 solvents are listed in Table 2, the deviations to the listed χ_E and χ_{DMA} values are the confidence interval (P = 0.95) for a given set of experimental spectra.

A comparison of Tables 1 and 2 demonstrates that for linear alkanes an increase in integral DMA emission S_{DMA} correlates with increasing luminescence quantum yield (φ_f) and excited state lifetime (τ_f) of the solvent. This clearly shows that generation of DMA excited states in this system proceeds mostly *via* direct energy transfer from an excited solvent molecule, which grows more efficient

Tab. 1: Physico-chemical and luminescent properties of the studied alkanes.

Solvent	η, cP[a]	μ·10⁴, cm²/(V·s)[b]	τ_f, ns[c]	$\varphi_f^{147}\cdot10^3$[d]	$\varphi_f^{165}\cdot10^3$[e]	λ_m, nm[f]
n-hexane	0.31	5.7	<0.7	0.2	0.6	206
n-heptane	0.42	–	1.1	0.7	1.6	206
n-octane	0.55	3.8	1.5	1.1	2.5	207
n-decane	0.91	2.4	3.0	2.0	4.2	207
n-dodecane	1.50	1.7	4.2	3.2	5.5	207
n-hexadecane	3.45	0.8	5.2	4.4	7.6	207
cyclohexane	0.98	1.9	1.1	3.5	8.8	201
methylcyclohexane	0.73	3.0	1.3	5.5	11.2	213
isooctane	0.51	3.6	<0.2	<0.01	<0.01	–
2,3-dimethylbutane	0.34	3.6	1.4	0.9	6.1	242
squalane	35.4	0.14	1.4	–	1.6	–

The table lists: [a]viscosity at 20 °C [132]; [b]mobility of tolane radical ions at 20 °C [133]; [c]excited state lifetime [81, 128] (squalane [130, 131]); [d]quantum yield of luminescence for excitation at 147 nm at 20 °C [80, 128]; [e]quantum yield of luminescence for excitation at 165 nm at 20 °C [80, 128]; [f]wavelength of maximum emission [80].

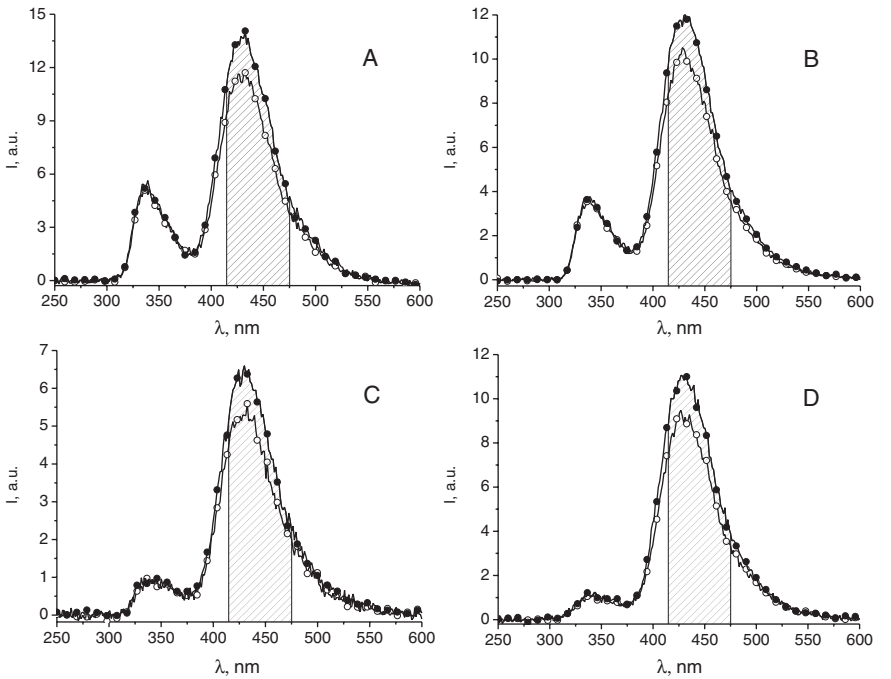

Fig. 8: Spectra of X-ray generated luminescence for a mixture of $6 \cdot 10^{-3}$ M 1-(phenylethynyl)-4-(trifluoromethyl)benzene and $1 \cdot 10^{-2}$ M DMA in different alkanes in applied magnetic field 20 mT (●) and in zero field (○): (A) *n*-decane, $\chi_E = 19.3 \pm 0.4\%$; (B) cyclohexane, $\chi_E = 17.3 \pm 0.5\%$; (C) 2,3-dimethylbutane, $\chi_E = 20.3 \pm 0.5\%$; (D) isooctane, $\chi_E = 19.1 \pm 0.5\%$. Magnetic field effect was determined in the marked wavelength range.

with increasing the emission lifetime and quantum yield of the solvent. On the other hand, as the viscosity of the linear alkane increases (by about an order of magnitude upon transition from *n*-hexane to *n*-hexadecane) the integral exciplex emission S_E remains constant, which confirms exciplex formation *via* diffusion-indifferent radical ion pair recombination. Furthermore, the magnitude of the magnetic field effect in the exciplex emission band is also practically identical for the entire set of the studied *n*-alkanes. The small χ_{DMA} in all alkanes under study is due to partial recombination of secondary radical ion pairs $D^{+\cdot}/A^{-\cdot}$ into DMA excited molecules. As was mentioned above generation of DMA excited states is also possible *via* nonmagnetosensitive direct energy transfer from an excited solvent molecule, that's why the magnitude of χ_{DMA} is rather small compared to χ_E, where all exciplexes are formed *via* recombination.

When cycloalkanes or squalane are used as the solvent the values χ_E drop by about 2–3% as compared to other alkanes which is a statistically reliable decrease.

Tab. 2: Magnetic field effects for the 1-(phenylethynyl)-4-(trifluoromethyl)benzene – DMA pair in 11 solvents.

Solvent	χ_E, %[a]	χ_{DMA}, %[b]	S_E, rel. u.[c]	S_{DMA}, rel. u.[d]
n-hexane	19.6 ± 0.7	4.4 ± 0.7	47 ± 3	5.1 ± 0.5
n-heptane	19.2 ± 0.2	3.3 ± 0.5	45 ± 6	7.6 ± 0.4
n-octane	19.4 ± 0.7	4.4 ± 0.9	52 ± 5	11 ± 2
n-decane	19.3 ± 0.4	3.8 ± 0.6	53 ± 4	16 ± 2
n-dodecane	19.8 ± 0.6	4.4 ± 0.8	51 ± 5	16 ± 2
n-hexadecane	19.4 ± 0.6	4.2 ± 0.6	54 ± 5	19 ± 2
cyclohexane	17.3 ± 0.5	3.7 ± 0.4	45 ± 5	11 ± 1
methylcyclohexane	16.2 ± 0.6	3.9 ± 0.9	27 ± 3	9.9 ± 0.5
isooctane	19.1 ± 0.5	4 ± 3	39 ± 3	2.7 ± 0.3
2,3-dimethylbutane	20.3 ± 0.5	3 ± 2	25 ± 3	3.3 ± 0.4
squalane	18.1 ± 0.6	5.8 ± 0.8	20 ± 3	13 ± 1

The table lists: [a]magnetic field effect in exciplex emission band (415–475 nm); [b]magnetic field effect in intrinsic DMA emission band (315–360 nm); [c]absolute area under the exciplex emission band (415–475 nm); [d]absolute area under the intrinsic DMA emission band (315–360 nm).

We also note that for branched alkanes, i.e. isooctane, 2,3-dimethylbutane, squalane, and methylcyclohexane, the absolute area under the exciplex emission band S_E is substantially lower than for linear alkanes, i.e. the number of forming exciplexes is smaller. A possible explanation is the known more efficient in comparison to *n*-alkanes formation of alkenes and products of C–C cleavage next to the branching site in the solvent radical cation, which reduces the number of solvent radical cations available for capturing, and thus the number of secondary radical ion pairs $D^{+\bullet}/A^{-\bullet}$ and the recombination exciplexes. Formation of alkenes as the products of alkane photolysis is also the quoted reason for different luminescence yields at different excitation wavelengths, *cf.* Table 1 [80]. The shorter wavelength excitation (147 nm instead of 165 nm) results in a more efficient photolysis and thus a higher concentration of photolysis products, which in turn effectively quench emission thus reducing the quantum yield of luminescence. As Table 1 demonstrates, the largest difference in quantum yields of luminescence for excitation at 147 nm and 165 nm is indeed observed for branched alkanes, which indirectly supports a more efficient decomposition of radical cations for branched alkanes in the conditions of X-irradiation. The work [128] reports quantum yields of photolysis products for isooctane, which are 0.08, 0.17, 0.36, and 0.05 for H_2, CH_4, C_4H_{10}, and C_5H_{10}, respectively. It is the efficient decomposition of an excited isooctane molecule that the authors attribute the very low emission yield of this alkane to. In a similar fashion, in ref. [131] the efficient decomposition of excited states of branched alkanes was called upon to rationalize the shortening of the

excited state lifetime of, e.g. squalane ($\tau_f = 1.4$ ns) in comparison to linear alkanes of comparable chain length, such as *n*-hexadecane ($\tau_f = 5.2$ ns). The possibility of efficient formation of alkenes and C–C cleavage products upon X-irradiation of isooctane was also discussed in refs. [134, 135]. Also radical cation of tetramethylethylene was identified to be the product of unimolecular decay of 2,3-dimethylbutane radical cation in low-temperature freon matrices [136, 137]. In ref. [138] one can find comprehensive investigation of branched alkanes cation radicals by means of TR MFE and their lifetime estimations.

The connection between the magnitude of the observed magnetic field effect and the fraction of spin-correlated radical ion pairs (4) can be obtained from expression (1) of ref. [139] by using the definition of θ given in ref. [134]:

$$\theta = \frac{\chi_E}{1-(4\rho_0-1)\cdot(\chi_E+1)}, \tag{4}$$

where θ is the fraction of spin-correlated pairs, χ_E is the magnitude of the magnetic field effects (in the studied system 1-(phenylethynyl)-4-(trifluoromethyl)benzene – DMA we determined it in the exciplex emission band), and ρ_0 is the equilibrium singlet state population of the pair in zero magnetic field. The value of ρ_0 depends on the situation, its limiting value of 1/4 corresponds to spin evolution completely contained within a single radical ion pair without any operating charge transfer processes [140]. Any processes of charge transfer between a radical ion and a neutral molecule accompanying the process of recombination result in increased ρ_0. For a single charge transfer upon transition of pair $S^{+\bullet}/A^{-\bullet}$ into pair $D^{+\bullet}/A^{-\bullet}$ by capturing solvent hole $S^{+\bullet}$ to a positive charge acceptor D the value of ρ_0 is equal to 5/18 [141]. Multiple charge transfer, typical for processes of degenerate charge exchange in concentrated solutions, result in the ρ_0 value of 1/3 [116]. Using these benchmark values of ρ_0 and the experimentally determined χ_E values, we can use expression (4) to obtain the fractions θ in the studied alkanes. For all alkanes except for cyclohexane, methylcyclohexane and squalane θ were calculated to be approximately 0.19 ± 0.01, 0.22 ± 0.01 and 0.32 ± 0.01 for ρ_0 of 1/4, 5/18 and 1/3, respectively. For the three outliers that all share in common the presence of fast solvent hole the values of θ are somewhat lower at 0.17 ± 0.01, 0.20 ± 0.01 and 0.28 ± 0.01, respectively. It is interesting to note that the values for isooctane do not significantly deviate from the values for linear alkanes, although it is known that the range of electron thermalization upon ionization for such "spherical" molecules as isooctane and neopentane is significantly larger than for regular *n*-alkanes [142].

The estimated θ values for a representative set of alkanes reasonably agree with available published data obtained by other techniques: TR MFE (a relatively

sophisticated experimental technique, typical θ values 0.2–0.4 [139, 143]), CW magnetic field effect for non-exciplex forming systems usually comprising a molecule that simultaneously captures both electron and solvent hole (a substantial contribution to emission from non-magnetosensitive channels of excitation generation that lowers magnetic field effect, typical θ values 0.1–0.3 [143–145]), analysis of Δg quantum beats in a special probe pair *p*-terphenyl-d_{14} – diphenylsulphide-d_{10} with substantially shifted g-values of the two pair radical ions [134, 146]. The latter technique is not sensitive to non-recombination processes and thus provides seemingly more reliable θ values, but it is directly applicable to a limited range of solvents that do not imprint substantial spin evolution in the solvent radical cation prior to its capture by the sulphur-centred radical cation, e.g. it yields θ = 0.26 for cyclohexane that satisfies this requirement, but θ = 0.19 for isooctane that has substantial hyperfine couplings in its radical cation that poorly average out by degenerate charge transfer [147, 148].

The estimated θ values should also be compared to θ = 0.28 for *n*-dodecane and 0.22 for cyclohexane, as determined in the previous section from TR MFE experiments in dilute solutions of **FT** in alkanes without introducing the second pair partner. It can be seen that these reference values fit well between the estimates of θ calculated for the situations of single and multiple charge transfer, which both are certainly present in the systems used to obtain the quoted χ_E values, reproducing the lower value for the cyclic alkane. We can therefore use the value of ρ_0 between 5/18 and 1/3 to estimate the value of θ from the measured values of χ_E, and can directly compare thus obtained estimates of θ for relative magnitudes and trends without the necessity to consider additional complications due to limited applicability of the more advanced techniques.

4 Conclusions and outlook

The suggested method to estimate the fraction of spin-correlated radical ion pairs θ by measuring the magnitude of magnetic field elect in the exciplex emission band in a donor-acceptor system with optimal luminescent properties of the forming excited complex is a relatively simple experimental technique applicable in any solvent, in which excited states can be generated *via* recombination of a radical ion pair, and in arbitrary concentrated solutions. On the other hand, the knowledge of θ is needed for correct interpretation of many experiments in radiation spin chemistry and for linking their results with calculated spin evolution in the radical ion pair. An important development of this approach is estimation of the fraction of spin-correlated pairs, and in a wider sense investigation

of spin-correlated radical pairs in other condensed systems as well, including polymer matrices. While in alkane solutions all obtained values of θ turned out to be rather close to each other and to the expected values, what would happen in polymers is not known. In this work we applied our approach to a set of solvents with viscosity differing by as much as two orders of magnitude (*n*-hexane to squalane), and the latter is already close to a model of an aliphatic polymer like polypropylene or polyisobutylene. Furthermore, as discussed in our earlier papers, radiation-induced recombination luminescence is a convenient model for electroluminescence in molecular systems, which forms the basis of modern all-organic optoelectronic devices, and exciplex formation can be used for spectral tuning of emission and improving optoelectric conversion efficiency of such devices by avoiding self-absorption within the device.

Acknowledgments: The work was supported by Russian Science Foundation (project no. 16-13-10163). A.R.M. is grateful to the Council for Grants of the President of the Russian Federation for awarding a personal scholarship for Support of Young Researchers (project no. SP-81.2016.1).

References

1. G. R. Eaton, S. S. Eaton, K. M. Salikhov, Foundations of Modern EPR. World Scientific (1998).
2. V. I. Feldman, Radiat. Phys. Chem. **55** (1999) 565.
3. A. D. Milov, K. M. Salikhov, M. D. Shirov, Sov. Phys. Solid State **23** (1981) 565.
4. A. D. Milov, K. M. Salikhov, Y. D. Tsvetkov, Chem. Phys. Lett. **8** (1971) 523.
5. A. A. Obynochny, A. G. Maryasov, P. A. Purtov, K. M. Salikhov, Appl. Magn. Reson. **15** (1998) 259.
6. W. K. Subczynski, J. S. Hyde, Biophys. J. **45** (1984) 743.
7. K. Toriyama, M. Iwasaki, K. Nunome, H. Muto, J. Chem. Phys. **75** (1981) 1633.
8. J. H. Ardenkjaer-Larsen, I. Laursen, I. Leunbach, G. Ehnholm, L.-G. Wistrand, J. S. Petersson, K. Golman, J. Magn. Reson. **133** (1998) 1.
9. H. M. Swartz, R. B. Clarkson, Phys. Med. Biol. **43** (1998) 1957.
10. Y. Iwasaki, T. Osasa, M. Asahi, M. Matsumura, Y. Sakaguchi, T. Suzuki, Phys. Rev. B. **74** (2006) 195209.
11. V. I. Krinichnyi, E. I. Yudanova, J. Phys. Chem. C. **116** (2012) 9189.
12. A. Schnegg, J. Behrends, M. Fehr, K. Lips, Phys. Chem. Chem. Phys. **14** (2012) 14418.
13. Y. Sheng, T. D. Nguyen, G. Veeraraghavan, Ö. Mermer, M. Wohlgenannt, S. Qiu, U. Scherf, Phys. Rev. B. **74** (2006) 045213.
14. E. G. Bagryanskaya, Y. A. Grishin, R. Z. Sagdeev, Y. N. Molin, Chem. Phys. Lett. **114** (1985) 138.
15. E. L. Frankevich, M. M. Tribel, I. A. Sokolik, A. I. Pristupa, Phys. Status Solidi B **87** (1978) 373.
16. Y. N. Molin, O. A. Anisimov, V. M. Grigor'yants, V. K. Molchanov, K. M. Salikhov, J. Phys. Chem. **84** (1980) 1853.
17. A. D. Trifunac, J. P. Smith, Chem. Phys. Lett. **73** (1980) 94.

18. K. M. Salikhov, Y. N. Molin, R. Z. Sagdeev, A. L. Buchachenko, Spin Polarization and Magnetic Effects in Radical Reactions, Netherlands, Elsevier (1984).
19. A. J. Hoff, Phys. Rep. **54** (1979) 75.
20. K. M. Salikhov, A. J. Van der Est, D. Stehlik, Appl. Magn. Reson. **16** (1999) 101.
21. M. C. Thurnauer, Rev. Chem. Intermed. **3** (1979) 197.
22. S. G. Zech, W. Lubitz, R. Bittl, Ber. Bunsen-Ges. Phys. Chem. **100** (1996) 2041.
23. K. M. Salikhov, J. H. Golbeck, D. Stehlik, Appl. Magn. Reson. **31** (2007) 237.
24. V. I. Borovkov, I. S. Ivanishko, V. A. Bagryansky, Y. N. Molin, J. Phys. Chem. A. **117** (2013) 1692.
25. K. L. Ivanov, M. V. Petrova, N. N. Lukzen, K. Maeda, J. Phys. Chem. A. **114** (2010) 9447.
26. J. A. Jones, K. Maeda, P. J. Hore, Chem. Phys. Lett. **507** (2011) 269.
27. P. A. Purtov, Chem. Phys. Lett. **496** (2010) 335.
28. A. I. Kruppa, T. V. Leshina, R. Z. Sagdeev, K. M. Salikhov, F. S. Sarvarov, Chem. Phys. **67** (1982) 27.
29. S. Richert, A. Rosspeintner, S. Landgraf, G. Grampp, E. Vauthey, D. R. Kattnig, J. Am. Chem. Soc. **135** (2013) 15144.
30. O. A. Anisimov, Ion Pairs in Liquids, (Eds. A. Lund, M. Shiotani), Netherlands, Springer, (1991), P. 285.
31. I. A. Shkrob, A. D. Trifunac, Radiat. Phys. Chem. **50** (1997) 227.
32. J. Klein, R. Voltz, Phys. Rev. Lett. **36** (1976) 1214.
33. Y. N. Molin, Bull. Korean Chem. Soc. **20** (1999) 7.
34. E. V. Kalneus, D. V. Stass, Y. N. Molin, Appl. Magn. Reson. **28** (2005) 213.
35. W. M. Bartczak, A. Hummel, J. Chem. Phys. **87** (1987) 5222.
36. V. V. Lozovoy, S. V. Anishchik, N. N. Medvedev, O. A. Anisimov, Y. N. Molin, Chem. Phys. Lett. **167** (1990) 122.
37. M. Wojcik, M. Witold, Bartczak, J. Kroh, Chem. Phys. Lett. **177** (1991) 184.
38. V. I. Borovkov, K. A. Velizhanin, Radiat. Phys. Chem. **76** (2007) 988.
39. V. I. Borovkov, K. A. Velizhanin, Radiat. Phys. Chem. 76 (2007) 998
40. A. R. Melnikov, E. V. Kalneus, V. V. Korolev, I. G. Dranov, A. I. Kruppa, D. V. Stass, Photochem. Photobiol. Sci. **13** (2014) 1169.
41. A. R. Melnikov, E. V. Kalneus, V. V. Korolev, I. G. Dranov, D. V. Stass, Dokl. Phys. Chem. **452** (2013) 257.
42. J. B. Birks, Nature **214** (1967) 1187.
43. E. A. Chandross, C. J. Dempster, J. Am. Chem. Soc. **92** (1970) 3586.
44. D. R. Kattnig, A. Rosspeintner, G. Grampp, Phys. Chem. Chem. Phys. **13** (2011) 3446.
45. N. L. Lavrik, J. Mol. Struct. **115** (1984) 477.
46. Y. H. Lee, M. Lee, Bull. Korean Chem. Soc. **18** (1997) 1054.
47. P. P. Levin, V. A. Kuz'min, B. Acad. Sci. USSR Ch. **35** (1986) 1303.
48. N. K. Petrov, V. N. Borisenko, M. V. Alfimov, T. Fiebig, H. Staerk, J. Phys. Chem. **100** (1996) 6368.
49. M. A. F. Tavares, Trans. Faraday Soc. **66** (1970) 2431.
50. M. Ottolenghi, Acc. Chem. Res. **6** (1973) 153.
51. A. J. Bard (Ed.), Electrogenerated Chemiluminescence, New York, Marcel Dekker Inc. (2004).
52. J. B. Ketter, R. M. Wightman, J. Am. Chem. Soc. **126** (2004) 10183.
53. A. Weller, K. Zachariasse, Chem. Phys. Lett. **10** (1971) 590.
54. V. I. Borovkov, I. S. Ivanishko, Radiat. Phys. Chem. **80** (2011) 540.
55. Y. Hirata, T. Okada, N. Mataga, T. Nomoto, J. Phys. Chem. **96** (1992) 6559.

56. C. Ferrante, U. Kensy, B. Dick, J. Phys. Chem. **97** (1993) 13457.
57. K. Bhattacharyya, M. Chowdhury, Chem. Rev. **93** (1993) 507.
58. P. P. Levin, P. F. Pluzhnikov, V. A. Kuzmin, Chem. Phys. Lett. **147** (1988) 283.
59. N. Mataga, H. Miyasaka, Electron Transfer and Exciplex Chemistry, in: Advances in Chemical Physics: Electron Transfer from Isolated Molecules to Biomolecules, Vol. 107 (Part 2)., (Eds. J. Jortner, M. Bixon), New York, Wiley (1999) 431.
60. D. N. Nath, M. Chowdhury, Chem. Phys. Lett. **109** (1984) 13.
61. N. K. Petrov, A. I. Shushin, E. L. Frankevich, Chem. Phys. Lett. **82** (1981) 339.
62. H. J. Werner, Z. Schulten, K. Schulten, J. Chem. Phys. **67** (1977) 646.
63. S. G. Fedorenko, A. I. Burshtein, J. Chem. Phys. **141** (2014) 114504.
64. S. P. Van, G. S. Hammond, J. Am. Chem. Soc. **100** (1978) 3895.
65. S. T. Cheung, W. R. Ware, J. Phys. Chem. **87** (1983) 466.
66. K. Sonogashira, Y. Tohda, N. Hagihara, Tetrahedron Lett. **16** (1975) 4467.
67. R. D. Stephens, C. E. Castro, J. Org. Chem. **28** (1963) 3313.
68. E. V. Kalneus, A. R. Melnikov, V. V. Korolev, V. I. Ivannikov, D. V. Stass, Appl. Magn. Reson. **44** (2013) 81.
69. Y. N. Molin, O. A. Anisimov, Radiat. Phys. Chem. **21** (1983) 77.
70. D. V. Stass, N. N. Lukzen, B. M. Tadjikov, Y. N. Molin, Chem. Phys. Lett. **233** (1995) 444.
71. S. V. Anishchik, V. M. Grigoryants, I. V. Shebolaev, Y. D. Chernousov, O. A. Anisimov, Y. N. Molin, Instrum. Exp. Tech. **32** (1990) 813.
72. V. I. Borovkov, S. V. Anishchik, O. A. Anisimov, Chem. Phys. Lett. **270** (1997) 327.
73. K. G. Thakur, G. Sekar, Synthesis **16** (2009) 2785.
74. J. Saltiel, V. R. Kumar, J. Phys. Chem. A. **116** (2012) 10548.
75. M. Wierzbicka, I. Bylinska, C. Czaplewski, W. Wiczk, RSC Adv. **5** (2015) 29294.
76. Y. Hirata, T. Okada, T. Nomoto, Chem. Phys. Lett. **209** (1993) 397.
77. K. Okuyama, T. Hasegawa, M. Ito, N. Mikami, J. Phys. Chem. **88** (1984) 1711.
78. A. M. Brouwer, Pure Appl. Chem. **83** (2011) 2213.
79. I. B. Berlman, Handbook of Fluorescence Spectra of Aromatic Molecules. New York, Academic Press (1971).
80. W. Rothman, F. Hirayama, S. Lipsky, J. Phys. Chem. **58** (1973) 1300.
81. K. Shinsaka, H. Koizumi, T. Yoshimi, N. Kouchi, Y. Nakamura, M. Toriumi, M. Morita, Y. Hatano, S. Asaoka, H. Nishimura, J. Phys. Chem. **83** (1985) 4405.
82. A. R. Melnikov, E. V. Kalneus, V. V. Korolev, P. S. Sherin, V. I. Borovkov, D. V. Stass, Photochem. Photobiol. Sci. **15** (2016) 767.
83. D. W. Tweeten, K. Lee, S. Lipsky, Int. J. Radiat. Appl. Instrum., Part C. Radiat. Phys. Chem. **34** (1989) 771.
84. H. T. Choi, J. A. Haglund, S. Lipsky, J. Phys. Chem. **87** (1983) 1583.
85. C. D. Jonah, M. C. Sauer Jr, Int. J. Rad. Appl. Instrum. Part C. Radiat. Phys. Chem. **34** (1989) 497.
86. J. M. Warman, K. Asmus, R. H. Schuler, J. Phys. Chem. **73** (1969) 931.
87. V. O. Saik, N. N. Lukzen, V. M. Grigoryants, O. A. Anisimov, A. B. Doktorov, Y. N. Molin, Chem. Phys. **84** (1984) 421.
88. V. A. Bagryansky, O. M. Usov, N. N. Lukzen, Y. N. Molin, Appl. Magn. Reson. **12** (1997) 505.
89. K. M. Salikhov, Y. N. Molin, J. Phys. Chem. **97** (1993) 13259.
90. K. M. Salikhov, Y. Sakaguchi, H. Hayashi, Chem. Phys. **220** (1997) 355.
91. B. M. Tadjikov, A. V. Astashkin, Y. Sakaguchi, Chem. Phys. Lett. **284** (1998) 214.
92. A. V. Koptyug, V. O. Saik, O. A. Animisov, Y. N. Molin, Chem. Phys. **138** (1989) 173.
93. L. R. Mursalimov, K. Salikhov, Appl. Magn. Reson. **21** (2001) 223.

94. Y. E. Kandrashkin, K. M. Salikhov, D. Stehlik, Appl. Magn. Reson. **12** (1997) 141.
95. Y. E. Kandrashkin, K. M. Salikhov, A. Van der Est, D. Stehlik, Appl. Magn. Reson. **15** (1998) 417.
96. V. V. Lozovoy, V. M. Grigoryants, O. A. Anisimov, Y. N. Molin, P. V. Schastnev, L. N. Shchegoleva, I. I. Bilkis, V. D. Shteingarts, Chem. Phys. **112** (1987) 463.
97. D. R. Duling, J. Magn. Reson. B. **104** (1994) 105.
98. K. Pal, G. Grampp, D. R. Kattnig, ChemPhysChem. **14** (2013) 3389.
99. Y. N. Molin, K. M. Salikhov, K. I. Zamaraev, Spin Exchange. Principles and Applications in Chemistry and Biology. Berlin, Springer-Verlag (1980).
100. D. V. Stass, N. N. Lukzen, B. M. Tadjikov, V. M. Grigoryantz, Y. N. Molin, Chem. Phys. Lett. **243** (1995) 533.
101. O. A. Anisimov, V. M. Grigoryants, S. V. Kiyanov, K. M. Salikhov, S. A. Sukhenko, Y. N. Molin, Theor. Exp. Chem. **18** (1983) 256.
102. V. N. Verkhovlyuk, S. V. Anishchik, Y. N. Molin, O. A. Anisimov, Mol. Phys. **113** (2015) 113.
103. M. Justinek, G. Grampp, S. Landgraf, P. J. Hore, N. N. Lukzen, J. Am. Chem. Soc. **126** (2004) 5635.
104. K. L. Ivanov, D. V. Stass, E. V. Kalneus, R. Kaptein, N. N. Lukzen, Appl. Magn. Reson. **44** (2013) 217.
105. S. A. Sukhenko, P. A. Purtov, K. M. Salikhov, Sov. J. Chem. Phys. **2** (1985) 29.
106. D. V. Stass, B. M. Tadjikov, Y. N. Molin, Chem. Phys. Lett. **235** (1995) 511.
107. V. O. Saik, A. E. Ostafin, S. Lipsky, J. Chem. Phys. **103** (1995) 7347.
108. B. M. Tadjikov, D. V. Stass, Y. N. Molin, Chem. Phys. Lett. **260** (1996) 529.
109. B. M. Tadjikov, D. V. Stass, Y. N. Molin, J. Phys. Chem. A. **101** (1997) 377.
110. B. M. Tadjikov, D. V. Stass, O. M. Usov, Y. N. Molin, Chem. Phys. Lett. **273** (1997) 25.
111. V. M. Grigoryants, S. D. McGrane, S. Lipsky, J. Chem. Phys. **109** (1998) 7354.
112. E. V. Kalneus, A. A. Kipriyanov, P. A. Purtov, D. V. Stass, Y. N. Molin, Appl. Magn. Reson. **30** (2006) 549.
113. E. V. Kalneus, D. V. Stass, K. L. Ivanov, Y. N. Molin, Mol. Phys. **104** (2006) 1751.
114. E. V. Kalneus, A. A. Kipriyanov, P. A. Purtov, D. V. Stass, Y. N. Molin, Dokl. Phys. Chem. **415** (2007) 170.
115. N. V. Sergey, V. N. Verkhovlyuk, E. V. Kalneus, V. V. Korolev, A. R. Melnikov, A. B. Burdukov, D. V. Stass, Y. N. Molin, Chem. Phys. Lett. **552** (2012) 32.
116. K. Schulten, P. G. Wolynes, J. Chem. Phys. **68** (1978) 3292.
117. N. E. Polyakov, P. A. Purtov, T. V. Leshina, M. B. Taraban, R. Z. Sagdeev, K. M. Salikhov, Chem. Phys. Lett. **129** (1986) 357.
118. P. A. Purtov, K. M. Salikhov, Theor. Exp. Chem. **23** (1987) 192.
119. V. N. Verkhovlyuk, D. V. Stass, N. N. Lukzen, Y. N. Molin, Chem. Phys. Lett. **413** (2005) 71.
120. V. A. Bagryansky, V. I. Borovkov, Y. N. Molin, Russ. Chem. Rev. **76** (2007) 493.
121. V. I. Borovkov, D. V. Stass, V. A. Bagryansky, Y. N. Molin, Study of Spin-Correlated Radical Ion Pairs in Irradiated Solutions by Optically Detected Epr and Related Techniques, (Eds. A. Lund, M. Shiotani), Springer International Publishing (2014), P. 629.
122. V. I. Borovkov, Radiat. Phys. Chem. **77** (2008) 1190.
123. V. I. Borovkov, V. A. Bagryansky, I. V. Yeletskikh, Y. N. Molin, Mol. Phys. **100** (2002) 1379.
124. S. J. Rzad, R. H. Schuler, A. Hummel, J. Chem. Phys. **51** (1969) 1369.
125. J. M. Warman, P. P. Infelta, M. P. De Haas, A. Hummel, Chem. Phys. Lett. **43** (1976) 321.
126. E. Zador, J. M. Warman, A. Hummel, Chem. Phys. Lett. **23** (1973) 363.
127. V. A. Bagryansky, O. M. Usov, V. I. Borovkov, T. V. Kobzeva, Y. N. Molin, Chem. Phys. **255** (2000) 237.

128. R. Hermann, R. Mehnert, L. Wojnárovits, J. Lumin. **33** (1985) 69.
129. F. B. Sviridenko, D. V. Stass, Y. N. Molin, Chem. Phys. Lett. **297** (1998) 343.
130. Y. Katsumura, Y. Yoshida, S. Tagawa, Y. Tabata, Radiat. Phys. Chem. **21** (1983) 103.
131. I. A. Shkrob, M. C. Sauer, A. D. Trifunac, J. Phys. Chem. **100** (1996) 5993.
132. V. M. Tatevski (Ed.): Physical-Chemical Properies of Individual Hydrocarbons, Gostoptekhizdat, Moscow (1960) (in Russian).
133. V. I. Borovkov, S. V. Anishchik, O. A. Anisimov, Radiat. Phys. Chem. **67** (2003) 639.
134. O. M. Usov, V. M. Grigoryants, B. M. Tadjikov, Y. N. Molin, Radiat. Phys. Chem. **49** (1997) 237.
135. D. W. Werst, M. F. Desrosiers, A. D. Trifunac, Chem. Phys. Lett. **133** (1987) 201.
136. T. Miyazaki, H. Tsuruta, Y. Fujitani, K. Fueki, J. Phys. Chem. **86** (1982) 970.
137. Y. Saitake, T. Miyazaki, Z. I. Kuri, J. Phys. Chem. **77** (1973) 2418.
138. V. I. Borovkov, P. A. Potashov, L. N. Shchegoleva, V. A. Bagryansky, Y. N. Molin, J. Phys. Chem. A. **111** (2007) 5839.
139. J. A. LaVerne, B. Brocklehurst, J. Phys. Chem. **100** (1996) 1682.
140. E. W. Knapp, K. Schulten, J. Chem. Phys. **71** (1979) 1878.
141. W. R. S. Appleton, B. Brocklehurst, Chem. Phys. Lett. **136** (1987) 199.
142. W. F. Schmidt, Can. J. Chem. **55** (1977) 2197.
143. B. Brocklehurst, Int. Rev. Phys. Chem. **4** (1985) 279.
144. R. S. Dixon, V. J. Lopata, Can. J. Chem. **57** (1979) 3023.
145. R. S. Dixon, F. P. Sargent, V. J. Lopata, E. M. Gardy, B. Brocklehurst, Can. J. Chem. **55** (1977) 2093.
146. S. V. Anishchik, O. M. Usov, O. A. Anisimov, Y. N. Molin, Radiat. Phys. Chem. **51** (1998) 31.
147. S. V. Anishchik, V. I. Borovkov, V. I. Ivannikov, I. V. Shebolaev, Y. D. Chernousov, N. N. Lukzen, O. A. Anisimov, Y. N. Molin, Chem. Phys. **242** (1999) 319.
148. V. N. Verkhovlyuk, V. A. Morozov, D. V. Stass, A. B. Doktorov, Y. N. Molin, Chem. Phys. Lett. **378** (2003) 567.

Supplemental Material: The online version of this article (DOI: 10.1515/zpch-2016-0819) offers supplementary material, available to authorized users.